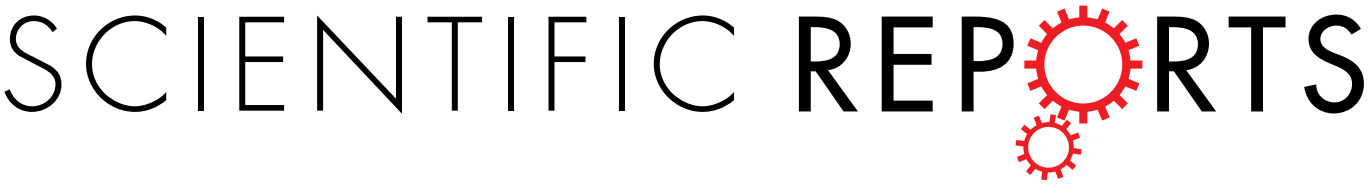

OPEN

Qubit-mediated deterministic nonlinear gates for quantum oscillators

Received: 12 May 2017
Accepted: 22 August 2017
Published online: 14 September 2017

Kimin Park, Petr Marek & Radim Filip

Quantum nonlinear operations for harmonic oscillator systems play a key role in the development of analog quantum simulators and computers. Since strong highly nonlinear operations are often unavailable in the existing physical systems, it is a common practice to approximate them by using conditional measurement-induced methods. The conditional approach has several drawbacks, the most severe of which is the exponentially decreasing success rate of the strong and complex nonlinear operations. We show that by using a suitable two level system sequentially interacting with the oscillator, it is possible to resolve these issues and implement a nonlinear operation both nearly deterministically and nearly perfectly. We explicitly demonstrate the approach by constructing self-Kerr and cross-Kerr couplings in a realistic situation, which require a feasible dispersive coupling between the two-level system and the oscillator.

Quantum computers or quantum Turing machines[1,2] take advantage of their quantum mechanical architecture and are capable of solving tasks which are exponentially hard for their classical counterparts[3–5]. Their predecessors are quantum simulators[6–8,9], which seek to emulate specific quantum dynamics of particular quantum systems in place of general processing. The fundamental principle of the simulations relies on mapping the complex quantum systems onto other more accessible and better controllable ones, such as trapped ions[10–13], photons[14,15], atomic lattices[16,17] and superconducting circuit[18,19]. The analog simulators are dedicated to continuous variables (CV) systems with infinite dimensional Hilbert space[20]. These systems allow for simulations of unexplored highly nonlinear open quantum dynamics[21–27]. Some CV nonlinear operations naturally appear in other physical systems, such as Bose-Einstein condensates[28], cold ions[29], or circuit quantum electrodynamics[30]. The spectrum of nonlinear operations is however limited and typically determined by the unique physics of specific experimental platforms.

A broader set of nonlinear operations for quantum harmonic oscillator can be elegantly realized by coupling them to suitable two-level systems (qubits)[31–35]. This realization is possible because the two-level systems are naturally nonlinear due to their saturability and offer a wide variety of qubit-oscillator couplings. The nonlinear nature in turn leads to dynamics of the oscillator which can be used for deterministic generation of nonclassical states[36] or for conditional realization of nonlinear quantum potentials[37,38]. The two level systems are also beneficial from a technical standpoint, allowing for a significantly larger number of individual interactions[39] than what is allowed for purely optical ancillary single photon states[40,41]. The conditional nature of these hybrid operations, however, limits them in their suitability for practical applications as well as quantum simulations, which ultimately leads to success rate exponentially decreasing with the number of operations involved.

In this report we propose a method for deterministic implementation of nonlinear unitary operations for quantum harmonic oscillators sequentially coupled to single qubits. This method relies on employing a sequence of available non-commuting qubit-oscillator interactions, similarly as in[23,42–44]. The qubits act only as mediators rather than for control unlike the conceptually similar quantum Zeno gates[45], starting and finishing the operation in a factorized state. The repeated gates incrementally create a Zeno-like nonlinear unitary dynamics deterministically and with a nearly unit fidelity. We illustrate the quality of the proposed method by explicitly analyzing realization of the self-Kerr and cross-Kerr nonlinearities done with help of a qubit sequentially coupled to the oscillator by dispersive interactions[46–52] under photon losses.

Department of Optics, Palacký University, 17. listopadu 1192/12, 77146, Olomouc, Czech Republic. Correspondence and requests for materials should be addressed to K.P. (email: park@optics.upol.cz)

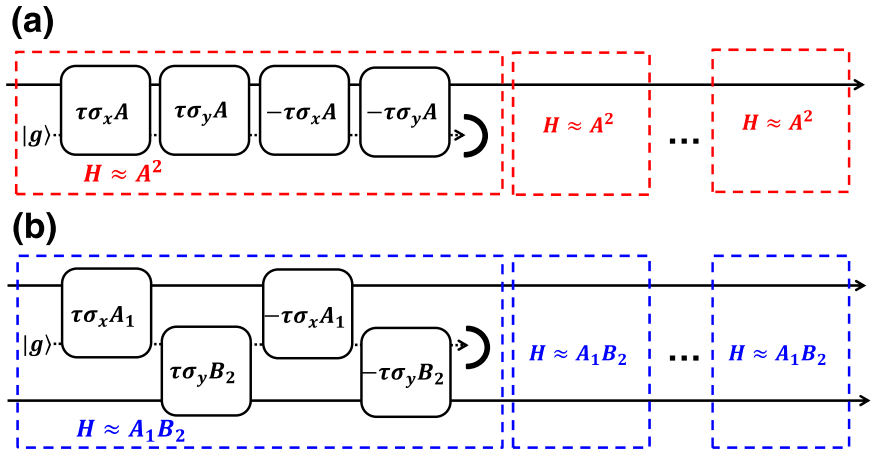

Figure 1. Concept of deterministic gates with oscillators mediated by a qubit where the interactions $H \approx \sigma_{x,y} A$, $H \approx \sigma_{x,y} A_1$ and $H \approx \sigma_{x,y} B_2$ between optical mode and ancillary mode are arranged to achieve a high-order nonlinearity: (**a**) scheme for single-mode optical interaction operator, and (**b**) scheme for a two-mode optical evolution operator. Each box with a written interaction Hamiltonian H represents the evolution $\exp[iH]$ for a unit of time, and the different colored boxes represent different operators acting on the ancillas. The ancillas prepared in a chosen state $|g\rangle$ are discarded after each set of interactions. Repetition of these unit approximate operators represented by dashed boxes makes high-strength operators.

Short-time oscillator interaction transduced by a qubit

Let us start by considering a short time evolution of a quantum oscillator mediated by a single qubit. The unitary oscillator-qubit interaction that enables the desired dynamics is governed by Hamiltonians of the type $H_{\hat{A}} = \hbar \hat{\sigma}_j \hat{A}$, where $\hat{\sigma}_j$ with $j = x, y, z$ relates to the qubit system and stands for one of Pauli matrices, and $\hat{A}$ is an operator acting on the oscillator. To achieve the desired gate on the oscillator, we can consider a pair of non-commuting unitary operators $\hat{U}_x = exp[i\tau\hat{\sigma}_x\hat{A}]$ and $\hat{U}_y = \exp[i\tau\hat{\sigma}_y\hat{B}]$ where the oscillator operators $\hat{A}$ and $\hat{B}$ commute $[\hat{A}, \hat{B}] = 0$. As depicted in Fig. 1a, we can join them into a sequence $\hat{U}_{xyxy} = \hat{U}_x\hat{U}_y\hat{U}_x^\dagger\hat{U}_y^\dagger$ following the idea of geometric phase effect[53]. In a manner similar to[23,54,55], this operator can be simplified to

$$\begin{aligned}\hat{U}_{xyxy} &= \exp[i\tau\hat{\sigma}_x\hat{A}]\exp[i\tau\hat{\sigma}_y\hat{B}]\exp[-i\tau\hat{\sigma}_x\hat{A}]\exp[-i\tau\hat{\sigma}_y\hat{B}] \\ &= 1 - 2\sin^2[\tau\hat{A}]\sin^2[\tau\hat{B}] + i\sin[2\tau\hat{A}]\sin^2[\tau\hat{B}]\hat{\sigma}_x \\ &\quad -i\sin^2[\tau\hat{A}]\sin[2\tau\hat{B}]\hat{\sigma}_y - \frac{i}{2}\sin[2\tau\hat{A}]\sin[2\tau\hat{B}]\hat{\sigma}_z \\ &\approx \exp[-2i\tau^2\hat{\sigma}_z\hat{A}\hat{B}] \equiv \hat{U}_{\hat{\sigma}_z\hat{A}\hat{B}},\end{aligned} \tag{1}$$

where the last line corresponds to a weak strength limit $\tau \ll 1$[56]. The resulting oscillator dynamics is driven by the product of operators $\hat{A}\hat{B}$ and coupled to the qubit by $\hat{\sigma}_z$. The qubit degree of freedom can be straightforwardly eliminated by preparing and measuring the qubit system in one of the relevant eigenstates, such as $|g\rangle$. The measurement then substitutes the discarding of qubit depicted in Fig. 1a. The whole sequence $\langle g|\hat{U}_{xyxy}|g\rangle$ then realizes a *conditional* operator

$$\hat{O}_1 = \langle g|\hat{U}_{xyxy}|g\rangle = 1 - 2\sin^2[\tau\hat{A}]\sin^2[\tau\hat{B}] + i\sin[2\tau\hat{A}]\sin[2\tau\hat{B}]/2, \tag{2}$$

which approximates unitary operation

$$U_{\hat{A}\hat{B}} = \exp[-2i\tau^2\hat{A}\hat{B}] \tag{3}$$

in the limit of small τ. The commutativity of $\hat{A}$ and $\hat{B}$ restricts the generality of the scheme, but still allows for many interesting cases. The base operators $\hat{A}$ and $\hat{B}$ can be compatible operators on a single oscillator (as in Fig. 1a), or different operations on two separate oscillators (illustrated in Fig. 1b). The most apparent scenarios in which the product of two operators is highly nontrivial and practically useful operation are the self-Kerr and cross-Kerr evolutions, which we will address in detail later.

Near-unitarity of short-time realistic interaction

The perfect operation (3) is realized only in the limit of short time $\tau \to 0$. However, we can increase the strength by repeating the individual operations. In each step, the ancillary qubit is initialized in the ground state, led to interact with the oscillator systems, and finally projected onto the ground state again. It does not matter whether a single physical qubit is used repetitively or if a number of different systems is employed. In any case, R repetitions realize quantum operation $\hat{O}_R = (\hat{O}_1)^R$ which approximates the ideal operation $\hat{O}_T \equiv e^{-2iR\tau^2\hat{A}\hat{B}}$. Interestingly

enough, in the limit of sufficiently small τ the re-initialization of qubit is not needed, as the approximate operator can be also obtained as $\hat{O}_R = \langle g|(\hat{U}_{xyxy})^R|g\rangle$.

For a specific test state $|\psi\rangle$, the performance of the operation can be quantified by looking at its successful implementation probability $P_s = \langle\psi|\hat{O}_R^\dagger\hat{O}_R|\psi\rangle$ and fidelity $F = |\langle\psi|\hat{O}_T^\dagger\hat{O}_R|\psi\rangle|^2/P_s$. These metrics inherently depend on the chosen state $|\psi\rangle$, but we can also directly analyze the sandwiched operators $\hat{Q}_f = \hat{O}_T^\dagger\hat{O}_R$ and $\hat{Q}_s = \hat{O}_R^\dagger\hat{O}_R$. In the ideal case of $\hat{O}_R = \hat{O}_T$, both of these operators $\hat{Q}_s$ and $\hat{Q}_f$ reduce to the identity operator 1. We can therefore discern the quality of the operation by looking at how far we are from this ideal scenario. This analysis is best accomplished by considering the joint eigenbasis of the commuting operators $\hat{A}$ and $\hat{B}$ consisting of states $|m\rangle$ with the respective eigenvalues m_A and m_B. Note that the basis does not need to be discrete. We can write the diagonal elements of $\hat{Q}_f$ and $\hat{Q}_s$ as

$$\left|\langle m|\hat{Q}_f|m\rangle\right|^2 = \langle m|\hat{O}_R^\dagger\hat{O}_T|m\rangle\langle m|\hat{O}_T^\dagger\hat{O}_R|m\rangle = \langle m|\hat{O}_R^\dagger|m\rangle\langle m|\hat{O}_R|m\rangle = \langle m|\hat{O}_R^\dagger\hat{O}_R|m\rangle = \langle m|\hat{Q}_s|m\rangle, \tag{4}$$

where the unitarity of the operator $\hat{O}_T$ and the commutativity between $\hat{O}_T$, $\hat{O}_R$ and $|m\rangle\langle m|$ is utilized. From (4), we may notice an interesting behavior: the fidelity and the success probability are not complementary and can approach unity *simultaneously*. This near-unitarity is the characteristic of schemes utilizing the qubit in the eigenstate of the realized operator as in (1). In the limit of small τ, the probability of success derived from (2) is expanded up to the lowest order as

$$\langle m|\hat{Q}_s|m\rangle \approx 1 - 4m_A^2m_B^2(m_A^2 + m_B^2)R\tau^6. \tag{5}$$

We can now use this expression to lower bound both the fidelity and the success probability for arbitrary quantum states. The operators $\hat{A}$ and $\hat{B}$ typically represent position, momentum, or number of quanta of the oscillators whose statistical distribution are asymptotically vanishing outside a certain range, and therefore are reasonably bounded in realistic physical systems. Any state can be expressed as the superposition $|\psi\rangle = \sum_m c_m|m\rangle$, and for a strictly bounded state, we can write $\sum_{m_A,m_B=0}^{m_{max}}|c_m|^2 = 1$ where $m_{max} = max(|m_A|, |m_B|)$ is the dimension(s) of the Hilbert space(s). The bounds for success probability and fidelity can be found as

$$\begin{aligned} P_s &= \sum_m |c_m|^2\langle m|\hat{Q}_s|m\rangle > \sum_m |c_m|^2\langle m_{max}|\hat{Q}_s|m_{max}\rangle = 1 - \varepsilon, \\ F &= \frac{1}{P_s}\left|\sum_m |c_m|^2\langle m|\hat{Q}_f|m\rangle\right|^2 > \left|\sum_m |c_m|^2|^2|\langle m_{max}|\hat{Q}_f|m_{max}\rangle\right|^2 = 1 - \varepsilon, \end{aligned} \tag{6}$$

where we used the fact that $\langle m|\hat{Q}_s|m\rangle$ is a decreasing function of m and the error bound is a function $\varepsilon(m_{max}, R, \tau) = 8m_{max}^6R\tau^6 = 4m_{max}^6T\tau^4 = m_{max}^6T^3/R^2 \ll 1$. Now as $\lim_{R\to\infty}\varepsilon = 0$ for any T and m_{max}, the error can be made arbitrarily small. For an arbitrarily chosen error bound ε and desired strength of the interaction T, a number of repetitions

$$R = \sqrt{\frac{m_{max}^6T^3}{\varepsilon}} \tag{7}$$

implements the desired operation with an error lower than ε.

Even for quantum states which are not sharply bounded, we can always find m'_{max} such that $\sum_{m_A,m_B=0}^{m'_{max}}|c_m|^2 = 1 - \varepsilon_2$ for any ε_2. With help of (6) we can now always lower bound the success probability and the fidelity by $P_S, F > 1 - \varepsilon - \varepsilon_2$, and we can again find R and m'_{max} such that the joint error $\varepsilon + \varepsilon_2$ is made arbitrarily small. We emphasize that the obtained bound is derived from the worst case scenario, and its main purpose lies in proving conceptual viability. In practical scenarios in which the approached quantum states are not centered at the boundary of the Hilbert space, the number of required repetitions can be significantly smaller.

The prominent aspect of our scheme is that its success probability can approach one even for many repetitions, implying that the measurement can be removed from the setup. We therefore follow the deterministic scheme depicted in Fig. 1. Formally, a single step of the operation is no longer represented by an operator $\hat{O}_1$, but by a trace preserving map which *deterministically* transforms any input state $\hat{\rho}_{in}$ into

$$\hat{\rho}_{out} = \mathrm{Tr}_q[\hat{U}_{xyxy}\{|g\rangle_q\langle g| \otimes \hat{\rho}_{in}\}\hat{U}_{xyxy}^\dagger] = \hat{O}_1\hat{\rho}_{in}\hat{O}_1^\dagger + \hat{O}_2\hat{\rho}_{in}\hat{O}_2^\dagger, \tag{8}$$

where $\hat{O}_1 = \langle g|\hat{U}_{xyxy}|g\rangle = 1 - 2\sin^2[\tau\hat{A}]\sin^2[\tau\hat{B}] + i\sin[2\tau\hat{A}]\sin[2\tau\hat{B}]/2$ is the successful operation and $\hat{O}_2 = \langle e|\hat{U}_{xyxy}|g\rangle = -\sin^2[\tau\hat{A}]\sin[2\tau\hat{B}] + i\sin[2\tau\hat{A}]\sin^2[\tau\hat{B}]$ is the erroneous operation. When the individual operation is repeated R times, the final output state can be expressed as

$$\hat{\rho}_{out} = P_s\hat{O}_R\hat{\rho}_{in}\hat{O}_R^\dagger + (1 - P_s)\hat{\rho}_{error}^R, \tag{9}$$

where P_s denotes the success probability of the probabilistic scheme with otherwise identical parameters and the density matrix $\hat{\rho}_{error}^R$ groups together all the realizations which would be in the probabilistic scenario disqualified by measurements. For states from Hilbert space limited by m_{max} the fidelity is lower bounded by

$$F \geq P_sF_c \approx 1 - 2\varepsilon. \tag{10}$$

This result shows that the performance of the deterministic scheme is comparable to the probabilistic regime. Considering the respective fidelities, the deterministic scheme achieves the performance of the probabilistic one when the number of repetitions R is increased by a factor of $\sqrt{2}$.

Example of self-Kerr quantum interaction

Let us explicitly demonstrate the performance of the proposed gate by realizing some of the nonlinear gates prevalent in quantum information theory and quantum technology. The self-Kerr operation[23,57] is realized by a unitary operator $\exp(iT\hat{n}^2)$ and in our approach it can be straightforwardly achieved by setting $\hat{A} = \hat{B} = \hat{n}$. The implementation requires coupling with Hamiltonian $H \propto \hat{n}\hat{\sigma}_j$, where σ_j are Pauli matrices. Such operations can be obtained from the Jaynes-Cummings Hamiltonian by diagonalizing it into the dispersive form $\omega_r\hat{n} + \Omega'\hat{\sigma}_z + g'\hat{\sigma}_z\hat{n}$[50] and eliminating the commuting local Hamiltonians by either by suitable strengths of the Hamiltonian constants $g' \gg \omega$, $g' \gg \Omega$, or applying suitable local operations. In the dispersive limit of the Jaynes-Cummings model, only a form of $\hat{\sigma}_z\hat{n}$ is available, but other operations can be achieved by performing suitable local rotations of the qubit: $e^{i\pi\hat{\sigma}_x/4}e^{i\tau\hat{\sigma}_z\hat{n}}e^{-i\pi\hat{\sigma}_x/4} = e^{i\tau\hat{\sigma}_y\hat{n}}$ and $e^{i\pi\hat{\sigma}_y/4}e^{i\tau\hat{\sigma}_z\hat{n}}e^{-i\pi\hat{\sigma}_y/4} = e^{-i\tau\hat{\sigma}_x\hat{n}}$. The realistic implementation in these systems therefore can be achieved by a qubit interacting with an oscillator in the dispersive regime, with intermittent qubit rotations in Bloch sphere and re-initialization back to ground state after each round. The operation can be also found in other physical systems: it can be obtained as a part of the dispersive interaction available between two-level systems and oscillators. The cavity field of a high finesse mirrors and the motional energy eigenstate of a thin dielectric membrane was used in the optomechanical setup[49]. The circular Rydberg states of Rb atoms and the Ramsey cavity field are coupled in this regime in cavity QED systems[46,47], and the cooper pair box qubit and the resonator field in 1D transmission line resonator are coupled in circuit QED systems[48,50].

In contrast to the approach of circuit QED[58], which employs suitable time-dependent driving of the qubit-oscillator, our method employs a set of identical elementary gates, which can be repeated in order to obtain strong interaction. As a consequence, the whole operation is less demanding from the point of view of the ability to control the employed quantum systems. The performance of the gate can be generally estimated from the parameters and from the available dimension given by m_{max}. However, such a bound may be too loose, and actual performance depends on the specific choice of the states. Let us apply the self-Kerr operation to a sample coherent state $|\beta\rangle = \exp[\beta\hat{a}^\dagger - \beta^*\hat{a}]|0\rangle$ with $\beta = 1$. The self-Kerr operation is non-classical and non-Gaussian operation, and produces a non-classical and non-Gaussian state when applied to a coherent state[59]. Such states are necessary for advanced application of quantum information processing such as quantum computation[60], and can be recognized by negative regions of their Wigner functions[61,62]. In relation to the self-Kerr effect a larger Kerr interaction strength T produces more complex structures of negative Wigner function[63,64].

In Fig. 2, we display the negative regions of Wigner function of self-Kerr transformed coherent states with various coupling parameters $T = 0.2, 0.4, 0.6, 0.8$. Apparently, a birth of highly nonclassical quantum interference in phase space can be observed. It is manifested by three separated regions of negativity. The figures show practically no difference between the ideal operation (above) and the deterministic approximate realization with $\tau = 0.02$ (middle). This observation is reinforced by a near unit fidelity $F = 1\text{–}0.8 \times 10^{-4}$ for $T = 0.8$. Interestingly, based on (10) and the parameters of the operation, the maximal Fock number corresponding to such a high bound of fidelity should be as small as $n_{max} = 2.06$, while only around 73% of the photons in the coherent state $|\beta = 1\rangle$ live in the subspace under 2. This again shows that the actual fidelity for general states can be higher than the bound given in (10). Coherent states $|\beta\rangle$ have an average photon number $\langle\hat{n}\rangle = |\beta|^2$ with an unclear maximum photon number. The fidelity for these states scales as $F \approx 1 - 9T^3|\beta|^{10}/R^2 = 1 - 36|\beta|^{10}T\tau^4 = 1 - 36\langle\hat{n}\rangle^5 T\tau^4$ for the lowest order expansion. Therefore we notice that these states have a smaller error in fidelity than the bound of errors scaling as n_{max}^6.

In realistic scenarios, the operation will have to endure the effects of imperfections, mainly the loss as the dominant decoherence model for quantum oscillators. The loss can be modeled by passively coupling the evolving system to a set of zero temperature oscillators. In our model, we consider a sequence of discrete couplings, one after each cycle of the elementary sequence (1). Each of these couplings transforms annihilation operator of the system as $\hat{a} \to \sqrt{\eta}\hat{a} + \sqrt{1-\eta}\hat{a}_{\text{bath}}$, where $\hat{a}_{\text{bath}}$ is annihilation operator of the auxiliary zero temperature oscillator which is immediately discarded. The single step transmittance parameter η strongly impacts the performance of the method. In order to see how large loss can the system actually tolerate, we have simulated the imperfect operation for $\eta = 1\text{–}5.6 \times 10^{-4}$, which corresponds to $\eta/2\tau^2 = 0.3$. The loss counteracts the effects of the nonlinear operation. As time of the interaction increases, the state is continuously becoming more and more non-classical, which is witnessed by the appearance of negative areas in its Wigner function. This is actually as high as the resilience of the setup goes, because when the loss is larger, the negativities in Wigner function are not observed. However, even in this case the loss is accumulated with time and at some point so much of the energy is lost that the non-classical features vanish. This can be seen in the bottom row of Fig. 2. We can see that while the loss of 13% of the energy for $T = 0.2$ did not severely affect the non-classicality, 40% loss for $T = 0.8$ removed one area of negativity. We therefore conclude that proposed method is not critically sensitive to basic decoherence caused by a loss in the oscillator.

Example of cross-Kerr quantum interaction

Another example of quantum nonlinear interactions is the cross-Kerr coupling between two harmonic oscillators. This gate is a key component in building important two-qubit single photon gates in linear optical quantum computation such as controlled NOT gates and Fredkin gates[65–67], and nondestructive photon detection[68,69]. It also enables direct photon-photon interaction used for many quantum information processing such as a one-way computation[70]. The cross-Kerr interaction, represented by a unitary operator $exp[iT\hat{n}_1\hat{n}_2]$, can be engineered from

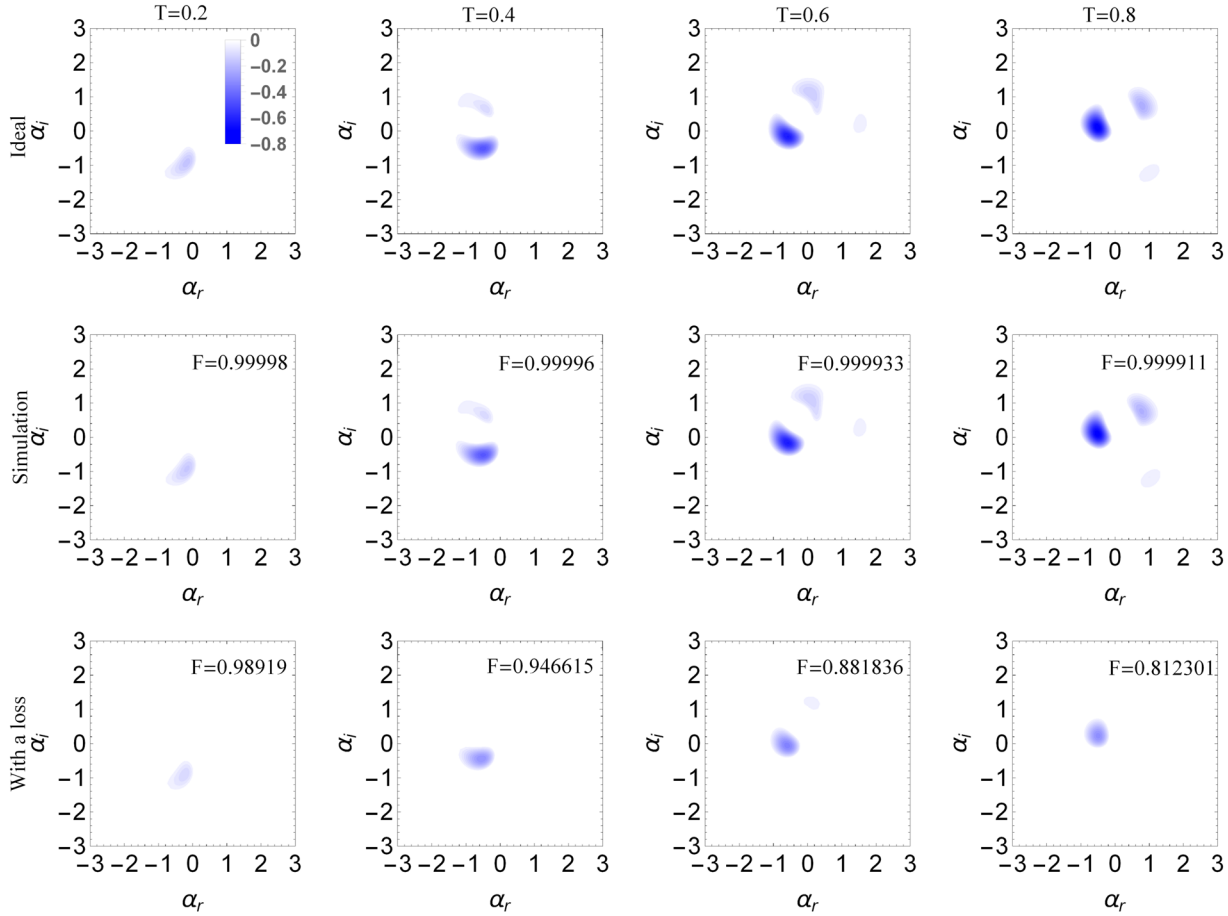

Figure 2. Negative regions of Wigner functions for coherent state $|\beta = 1\rangle$ subjected to self-Kerr interaction with total strengths $T = 0.2$ (first column), $T = 0.4$ (second column), $T = 0.6$ (third column), and $T = 0.8$ (fourth column). The top row shows the ideal realization of the operation, the middle row shows simulations with single step strength of $\tau = 0.02$, and the bottom row shows realistic lossy simulation with repeated single step transmittance $\eta = 1–5.6 \times 10^{-4}$. Insets show fidelities of the states with the ideal versions. We can see that the simulations faithfully recreate the ideal Wigner functions, even under the effects of moderate loss.

the same fundamental component as the self-Kerr operation: the dispersive coupling between an oscillator and a qubit, only this time the qubit is coupled to two separate oscillators (as in Fig. 1b) so $\hat{A} = \hat{n}_1$ and $\hat{B} = \hat{n}_2$. The two dispersive interactions $\exp[\pm i\tau\sigma_x\hat{n}_1]$ and $\exp[\pm i\tau\sigma_y\hat{n}_2]$ should be applied alternatingly being turned on and off by drive laser beams[47,50].

An elementary application is altering phase of a single photon based on the presence or absence of another, which is the basis for many discrete computation gates[65–67,71]. In an example of the control-Z gate[71], a separable state of two oscillators $|00\rangle + |01\rangle + |10\rangle + |11\rangle$ is changed to entangled state $|00\rangle + |01\rangle + |10\rangle - |11\rangle$ by the cross-Kerr gate with a strength $T = \pi$. Within our approach, the deterministic cross-Kerr gate with fidelity $F = 1–10^{-5}$ can be achieved from $R = 1000$ instances of the basic block. This scenario suits the approximation well due to a limited number of photons in the systems.

However, there are other applications in which larger photon numbers are significant[68,69]. To test for this scenario, we consider the cross-Kerr coupling between two coherent states with amplitudes $\alpha = \beta = 1$. Considering again interaction strength $T = \pi$, the operation can be implemented with fidelity $F = 0.989$ for $R = 1000$ and $F = 1–5 \times 10^{-4}$ with $R = 2500$ repetitions. A higher number of individual operations is demanded by the larger Hilbert space of the states for a fidelity comparable with the previous example. We can also analyze the operation from the point of view of entanglement it generates. There are several measures of entanglement[72], and here we adopt the negativity due to the ease of its evaluation[73]. The negativity of a bipartite state given by a density operator ρ can be obtained as $N[\rho] = \frac{\mathrm{Tr}[|\rho^{\mathrm{PT}}|] - 1}{2}$ as the measure of entanglement, where ρ^{PT} is the partial transposed density matrix and $\mathrm{Tr}[|\cdot|]$ is the trace norm. The analysis should also clearly show that the cross-Kerr gate is non-Gaussian and the created entanglement should therefore be of the non-Gaussian nature. To that end we also look at the Gaussian negativity $N_G[\rho] = \frac{\mathrm{Tr}\left[\left|\rho_G^{\mathrm{PT}}\right|\right] - 1}{2}$, where ρ_G is the density matrix of a Gaussian state which has all first and second moments of quadrature operators identical with ρ[74,75]. Both the Gaussian and the non-Gaussian entanglement of the state generated by the cross-Kerr gate are plotted in Fig. 3 for various values of

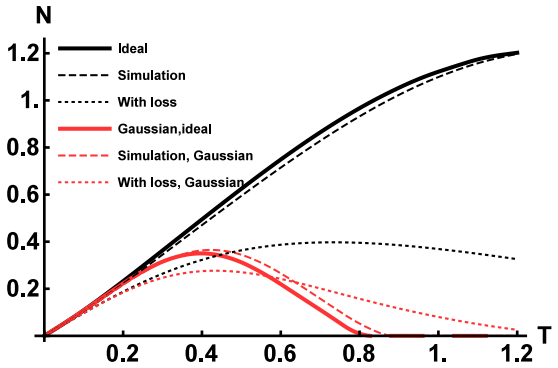

Figure 3. Entanglement generated by cross-Kerr gates with different strength T on a pair of coherent states $|\alpha\rangle_1|\beta\rangle_2$ with ideal cross-Kerr operator and the one achieved by our method with $\tau = 0.05$. We can see that for $T > 0.8$, the entanglement is purely non-Gaussian. When both oscillators suffer from loss with $\eta = 1\text{–}3.5 \times 10^{-3}$, we observe both reduction of overall entanglement and increase of Gaussian entanglement. This is the consequence of the loss drawing both states towards the pointer Gaussian vacuum state and Gaussifying them in the process. However, even under the effects of loss, purely non-Gaussian entanglement can still be obtained.

the interaction strength T. The interaction strength of dispersive interactions was chosen as $\tau = 0.05$. We can see that the entanglement created for larger values of T is practically completely non-Gaussian, as expected, and that the simulated process closely follows the ideal scenario.

To assess an impact of the decoherence on the cross Kerr interaction, we introduce an equal loss in the both oscillators. Simulations with a realistic loss with $\eta = 1\text{–}3.5 \times 10^{-3}$, corresponding to the same level of noise as in a previous section, show results conceptually similar to the self-Kerr case. Again, the loss limits the achievable number of elementary gates and the corresponding total interaction strength. State with dominantly non-Gaussian entanglement can be still achieved, but the maximal difference between non-Gaussian and Gaussian entanglement is limited. For our simulation, this difference $\max_\rho\{N[\rho] - N_G[\rho]\}$ was 0.31 at the energy loss of about 40% for a single arm. There is, however, another interesting effect. In addition to reducing the overall correlations, the loss also drives the quantum state towards Gaussianity. As a consequence, there is less of entanglement, but higher portion of it is Gaussian. In fact, for certain values of parameters the lossy scenario produces more Gaussian entanglement than the ideal one, while non-Gaussian nature is still accessible. It supports previous statements about a sufficient robustness of the method to the loss in oscillator.

Applications and outlook

In summary, using a single qubit as a recyclable mediator allows for synthesis of high order nonlinear operations on quantum oscillators. These operations can be realized at an arbitrary strength with both fidelity and probability of success approaching one. The only cost is represented by the required number of repetitions of the basic building block, which may be mitigated by using an optimized architecture. Operations which can be implemented depend on the available qubit-oscillator couplings. With the feasible dispersive coupling[46–52,76] it is possible to realize self-Kerr and cross-Kerr operations, which play a significant role in quantum information processing, with high quality under a moderate level of environmental effects. The extension of the scheme ranges from engineering high order quadrature nonlinear operators, such as cubic-phase gate operator by Rabi interactions[77–81], to hybrid interaction operator such as principally nonlinear optomechanical interactions[82–93] by combination of the dispersive and Rabi interactions. The higher-order versions of both dispersive and Rabi interactions open a broad class of CV nonlinear interactions. The involved harmonic oscillators can be physically varied (optical, mechanical, electrical, collective spins), and therefore this method can potentially provide wide class of nonlinear gates between these platforms. All of these potential applications open up a possibility of deterministic quantum simulators.

References

1. Benioff, P. The computer as a physical system: A microscopic quantum mechanical Hamiltonian model of computers as represented by Turing machines. *J. Stat. Phys.* **22**, 563 (1980).
2. Deutsch, D. Quantum theory, the Church-Turing principle and the universal quantum computer. *P. Roy. Soc. Lond. A.* **400**, 97 (1985).
3. Shor, P. W. Polynomial-time algorithms for prime factorization and discrete logarithms on a quantum computer. *SIAM J. Comput.*, **26**, 1484 (1997).
4. Simon, D. R. On the power of quantum computation. *Foundations of Computer Science, 1994 Proceedings., 35th Annual Symposium on:* 116 (1994).
5. Deutsch, D. & Jozsa, R. Rapid solution of problems by quantum computation. *P. Roy. Soc. Lond. A.* **439**, 553 (1992).
6. Kendon, V. M., Nemoto, K. & Munro, W. J. Quantum analogue computing. *Philos. Trans. R. Soc. Lond. A* **368**, 3609 (2010).
7. Cirac, J. I. & Zoller, P. Quantum computations with cold trapped ions. *Phys. Rev. Lett.* **74**, 4091 (1995).
8. Georgescu, I. M., Ashhab, S. & Nori, F. Quantum simulation. *Rev. Mod. Phys.* **86**, 153 (2014).
9. Feynman, R. P. Simulating physics with computers. *Int. J. Theor. Phys.* **21**, 467 (1982).
10. Kim, K. *et al.* Quantum simulation of the transverse Ising model with trapped ions. *Nature* **465**, 590 (2010).
11. Gerritsma, R. *et al.* Quantum simulation of the Dirac equation. *Nature* **463**, 68 (2010).
12. Lanyon, B. P. *et al.* Universal digital quantum simulation with trapped ions. *Science* **334**, 57 (2011).

13. Blatt, R. & Roos, C. F. Quantum simulations with trapped ions. *Nat. Phys.* **8**, 277 (2012).
14. Peruzzo, A. *et al*. Quantum walks of correlated photons. *Science* **329**, 1500 (2010).
15. Aspuru-Guzik, A. & Walther, P. Photonic quantum simulators. *Nat. Phys.* **8**, 285 (2012).
16. Simon, J. *et al*. Quantum simulation of antiferromagnetic spin chains in an optical lattice. *Nature* **472**, 307 (2011).
17. Bloch, I., Dalibard, J. & Nascimbéne, S. Quantum simulations with ultracold quantum gases. *Nat. Phys.* **8**, 267 (2012).
18. Houck, A. A., Türeci, H. E. & Koch, J. On-chip quantum simulation with superconducting circuits. *Nat. Phys.* **8**, 292 (2012).
19. Devoret, M. H. & Schoelkopf, R. J. Superconducting circuits for quantum information: an outlook. *Science* **339**, 1169–1174 (2013).
20. Braunstein, S. L. & van Loock, P. Quantum information with continuous variables. *Rev. Mod. Phys.* **77**, 513 (2005).
21. Filip, R., Marek, P. & Andersen, U. L. Measurement-induced continuous-variable quantum interactions. *Phys. Rev. A* **71**, 042308 (2005).
22. Miwa, Y. *et al*. Exploring a new regime for processing optical qubits: squeezing and unsqueezing single photons. *Phys. Rev. Lett.* **113**, 013601 (2014).
23. Lloyd, S. & Braunstein, S. L. Quantum computation over continuous variables. *Phys. Rev. Lett.* **82**, 1784 (1999).
24. Spiller, T. P. *et al*. Quantum computation by communication. *New J. Phys.* **8**, 30 (2006).
25. Gottesman, D., Kitaev, A. & Preskill, J. Encoding a qubit in an oscillator. *Phys. Rev. A* **64**, 012310 (2001).
26. Marek, P., Filip, R. & Furusawa, A. Deterministic implementation of weak quantum cubic nonlinearity. *Phys. Rev. A* **84**, 053802 (2011).
27. Miyata, K. *et al*. Implementation of a quantum cubic gate by an adaptive non-Gaussian measurement. *Phys. Rev. A* **93**, 022301 (2016).
28. Sefi, S. & van Loock, P. How to decompose arbitrary continuous-variable quantum operations. *Phy. Rev. Lett.* **107**, 170501 (2011).
29. Sefi, S., Vaibhav, V. & van Loock, P. Measurement-induced optical Kerr interaction. *Phys. Rev. A* **88**, 012303 (2013).
30. Yukawa, M. *et al*. Emulating quantum cubic nonlinearity. *Phys. Rev. A* **88**, 053816 (2013).
31. Greiner, M., Mandel, O., Hänsch, T. W. & Bloch, I. Collapse and revival of the matter wave field of a Bose-Einstein condensate. *Nature* **419**, 51 (2002).
32. Roos, C. F. *et al*. Nonlinear coupling of continuous variables at the single quantum level. *Phys. Rev. A* **77**, 040302(R) (2008).
33. Kirchmair, G. *et al*. Observation of quantum state collapse and revival due to the single-photon Kerr effect. *Nature* **495**, 205 (2013).
34. Leibfried, D., Blatt, R., Monroe, C. & Wineland, D. Quantum dynamics of single trapped ions. *Rev. Mod. Phys.* **75**, 281 (2003).
35. Xiang, Z. L., Ashhab, S., You, J. Q. & Nori, F. Hybrid quantum circuits: Superconducting circuits interacting with other quantum systems. *Rev. Mod. Phys.* **85**, 623 (2013).
36. Aspelmeyer, M., Kippenberg, T. J. & Marquardt, F. Cavity optomechanics. *Rev. Mod. Phys.* **86**, 1391 (2014).
37. Reiserer, A. & Rempe, G. Cavity-based quantum networks with single atoms and optical photons. *Rev. Mod. Phys.* **87**, 1379 (2015).
38. Lodahl, P., Mahmoodian, S. & Stobbe, S. Interfacing single photons and single quantum dots with photonic nanostructures. *Rev. Mod. Phys.* **87**, 347 (2015).
39. Marek, P., Lachman, L., Slodička, L. & Filip, R. Deterministic nonclassicality for quantum-mechanical oscillators in thermal states. *Phys. Rev. A* **94**, 013850 (2016).
40. Park, K., Marek, P. & Filip, R. Conditional nonlinear operations by sequential Jaynes-Cummings interactions. *Phys. Rev. A* **94**, 012332 (2016).
41. Park, K., Marek, P. & Filip, R. Finite approximation of unitary operators for conditional analog simulators. *Phys. Rev. A* **94**, 062308 (2016).
42. Sayrin, C. *et al*. Real-time quantum feedback prepares and stabilizes photon number states. *Nature* **477**, 73 (2011).
43. Fiurášek, J. Engineering quantum operations on traveling light beams by multiple photon addition and subtraction. *Phys. Rev. A* **80**, 053822 (2009).
44. Park, K., Marek, P. & Filip, R. Nonlinear potential of a quantum oscillator induced by single photons. *Phys. Rev. A* **90**, 013804 (2014).
45. Lloyd, S. Hybrid quantum computing. arXiv: quant-ph/0008057 (2000).
46. Huang, Y. P. & Moore, M. G. Interaction-and measurement-free quantum Zeno gates for universal computation with single-atom and single-photon qubits. *Phys. Rev. A* **77**, 062332 (2008).
47. Gleyzes, S. *et al*. Quantum jumps of light recording the birth and death of a photon in a cavity. *Nature* **446**, 297 (2007).
48. Guerlin, C. *et al*. Progressive field-state collapse and quantum non-demolition photon counting. *Nature* **448**, 889 (2007).
49. Schuster, D. I. *et al*. Resolving photon number states in a superconducting circuit. *Nature* **445**, 515 (2007).
50. Thompson, J. D. *et al*. Strong dispersive coupling of a high-finesse cavity to a micromechanical membrane. *Nature* **452**, 72 (2008).
51. Blais, A., Huang, R. S., Wallraff, A., Girvin, S. M. & Schoelkopf, R. J. Cavity quantum electrodynamics for superconducting electrical circuits: An architecture for quantum computation. *Phys. Rev. A* **69**, 062320 (2004).
52. Wallraff, A. *et al*. Circuit quantum electrodynamics: Coherent coupling of a single photon to a Cooper pair box. *Nature* **431**, 162 (2004).
53. Johnson, B. R. *et al*. Quantum non-demolition detection of single microwave photons in a circuit. *Nat. Phys.* **6**, 663 (2010).
54. Berry, M. V. Quantal phase factors accompanying adiabatic changes. *Proc. Roy. Soc. A* **392**, 45 (1984).
55. Aharonov, Y. & Anandan, J. Phase change during a cyclic quantum evolution. *Phys. Rev. Lett.* **58**, 1593 (1987).
56. van Loock, P. Optical hybrid approaches to quantum information. *Laser Photonics Rev.* **5**, 167 (2010).
57. The details of derivation are presented in Supplementary material.
58. Turchette, Q. A., Hood, C. J., Lange, W., Mabuchi, H. & Kimble, H. J. Measurement of conditional phase shifts for quantum logic. *Phys. Rev. Lett.* **75**, 4710 (1995).
59. Boca, A. *et al*. Observation of the Vacuum Rabi Spectrum for One Trapped Atom. *Phys. Rev. Lett.* **93**, 233603 (2004).
60. Krastanov, S. *et al*. Universal control of an oscillator with dispersive coupling to a qubit. *Phys. Rev. A* **92**, 040303 (R) (2015).
61. Weedbrook, C. *et al*. Gaussian quantum information. *Rev. Mod. Phys.* **84**, 621 (2012).
62. Wang, X. B., Hiroshima, T., Tomita, A. & Hayashi, M. Quantum information with Gaussian states. *Phys. Rep.* **448**, 1 (2007).
63. Jeong, H. & Kim, M. S. Efficient quantum computation using coherent states. *Phys. Rev. A* **65**, 042305 (2002).
64. Ralph, T. C., Gilchrist, A., Milburn, G. J., Munro, W. J. & Glancy, S. Quantum computation with optical coherent states. *Phys. Rev. A* **68**, 042319 (2003).
65. Kok, P. Effects of self-phase-modulation on weak nonlinear optical quantum gates. *Phys. Rev. A* **77**, 013808 (2008).
66. Stobińska, M., Milburn, G. J. & Wódkiewicz, K. Wigner function evolution of quantum states in the presence of self-Kerr interaction. *Phys. Rev. A* **78**, 013810 (2008).
67. Nemoto, K. & Munro, W. J. Nearly deterministic linear optical controlled-NOT gate. *Phys. Rev. Lett.* **93**, 250502 (2004).
68. Milburn, G. J. Quantum optical Fredkin gate. *Phys. Rev. Lett.* **62**, 2124 (1989).
69. Chuang, I. L. & Yamamoto, Y. Simple quantum computer. *Phys. Rev. A* **52**, 3489 (1995).
70. Imoto, N., Haus, H. A. & Yamamoto, Y. Quantum nondemolition measurement of the photon number via the optical Kerr effect. *Phys. Rev. A* **32**, 2287 (1985).
71. Munro, W. J., Nemoto, K., Beausoleil, R. G. & Spiller, T. P. High-efficiency quantum-nondemolition single-photon-number-resolving detector. *Phys. Rev. A* **71**, 033819 (2005).
72. Hutchinson, G. D. & Milburn, G. J. Nonlinear quantum optical computing via measurement. *J. Mod. Opt.* **51**, 1211 (2004).
73. Kok, P. *et al*. Linear optical quantum computing with photonic qubits. *Rev. Mod. Phys.* **79**, 135 (2007).
74. Wootters, W. K. Entanglement of Formation of an Arbitrary State of Two Qubits. *Phys. Rev. Lett.* **80**, 2245 (1998).

75. Hayden, P. M., Horodecki, M. & Terhal, B. M. The asymptotic entanglement cost of preparing a quantum state. *J. Phys. A: Math. Gen.* **34**, 6891 (2001).
76. Vidal, G. & Werner, R. F. Computable measure of entanglement. *Phys. Rev. A* **65**, 032314 (2002).
77. Laurat, J. *et al*. Entanglement of two-mode Gaussian states: characterization and experimental production and manipulation. *J. Opt. B: Quantum Semiclassical Opt.* **7**, S577 (2005).
78. Casanova, J., Romero, G., Lizuain, I., García-Ripoll, J. J. & Solano, E. Deep strong coupling regime of the Jaynes-Cummings model. *Phys. Rev. Lett.* **105**, 263603 (2010).
79. De Liberato, S. Light-matter decoupling in the deep strong coupling regime: The breakdown of the Purcell effect. *ibid* **112**, 016401 (2014).
80. Mezzacapo, A. *et al*. Digital Quantum Rabi and Dicke Models in Superconducting Circuits. *Sci. Rep* **4**, 7482 (2014).
81. Kienzler, D. *et al*. Observation of quantum interference between separated mechanical oscillator wave packets. *Phys. Rev. Lett.* **116**, 140402 (2016).
82. Sillanpää, M. A., Park, J. I. & Simmonds, R. W. Coherent quantum state storage and transfer between two phase qubits via a resonant cavity. *Nature* **449**, 438 (2007).
83. Günter, G. *et al*. Sub-cycle switch-on of ultrastrong light-matter interaction. *ibid* **458**, 178 (2009).
84. Niemczyk, T. *et al*. Circuit quantum electrodynamics in the ultrastrong-coupling regime. *Nat. Phys* **6**, 772 (2010).
85. Forn-Díaz, P. *et al*. Observation of the Bloch-Siegert shift in a qubit-oscillator system in the ultrastrong coupling regime. *Phys. Rev. Lett.* **105**, 237001 (2010).
86. Baust, A. *et al*. Ultrastrong coupling in two-resonator circuit QED. *Phys. Rev. B* **93**, 214501 (2016).
87. Aspelmeyer, M., Kippenberg, T. J. & Marquardt, F. *Cavity Optomechanics* (Berlin, Springer-Verlag, 2014).
88. Jayich, A. M. *et al*. Dispersive optomechanics: a membrane inside a cavity. *New J. Phys.* **10**, 095008 (2008).
89. Nunnenkamp, A., Børkje, K., Harris, J. G. E. & Girvin, S. M. Cooling and squeezing via quadratic optomechanical coupling. *Phys. Rev. A* **82**, 021806(R) (2010).
90. Sankey, J. C., Yang, C., Zwickl, B. M., Jayich, A. M. & Harris, J. G. E. Strong and tunable nonlinear optomechanical coupling in a low-loss system. *Nat. Phys* **6**, 707 (2010).
91. Liao, J.-Q. & Nori, F. Single-photon quadratic optomechanics. *Sci. Rep* **4**, 6302 (2014).
92. Lee, D. *et al*. Multimode optomechanical dynamics in a cavity with avoided crossings. *Nat. Commun.* **6**, 6232 (2014).
93. Park, K., Marek, P. & Filip, R. All-optical simulations of nonclassical noise-induced effects in quantum optomechanics. *Phys. Rev. A* **92**, 033813 (2015).

Acknowledgements

We acknowledge Project GB14-36681G of the Czech Science Foundation. K.P. acknowledges support by the Development Project of Faculty of Science, Palacký University.

Author Contributions

K.P. conceived the theory. P.M. and R.F. conceived the quantification, interpreted the implications and extended the scope. P.M. and R.F. led the project. All authors analyzed the results, wrote the article, and reviewed the manuscript.

Additional Information

Supplementary information accompanies this paper at doi:10.1038/s41598-017-11353-3

Competing Interests: The authors declare that they have no competing interests.

Publisher's note: Springer Nature remains neutral with regard to jurisdictional claims in published maps and institutional affiliations.